TECHNICAL ARTICLE—PEER-REVIEWED

Experimental Study on Frictional Pairs of Piston Pumps

Liqiang Xu (iD) · **Yuanhui Lu · Qingrui Liu · Lekang Lin ·
Jianhui Mu**

Abstract   To improve the service life and total efficiency
of the piston pumps, an alloy steel of HMn58-2 manganese
brass and 20CrMo are used as the material for a pin–disc,
and the change in the coefficient of friction of the pin–disc
is investigated via a friction/wear experiment. A Plint TE-
92 tribometer is used to conduct dry and wet wear exper-
iments on the pin–disc. After the experiments, the friction
and macroscopic morphology of the sample are analysed.
Results show that the wear in the dry friction experiment is
not uniform, the coefficient of friction increases quickly,
and the sample wears and fails. When using No. 46 anti-
wear hydraulic oil as the lubricant in the friction test, the
increase rate of the coefficient of friction is significantly
lower than that in the dry friction test. At a rotational speed
of 2,000 rpm and a load of 1.1 KN, the maximum coeffi-
cient of friction is 0.147. When the load is increased to
1,300 or 1,400 N and the speed is 1,600–2,000 rpm, the
coefficient of friction is greater than 0.011. A higher
rotational speed results in a smaller coefficient of friction,
whereas a greater load results in a higher coefficient of
friction, using lubricating oil can significantly reduce the
coefficient of friction. The effect of rotational speed on the
coefficient of friction is greater than the effect of load.

Keywords   Piston pump · Efficiency · Tribometer ·
Coefficient of friction

Introduction

In industrial production, mechanical parts experience fric-
tion and wear during motion; consequently, heat is
generated and the lifetime, reliability, and power con-
sumption of the machine are affected [1]. Wear is an
important topic that cannot be disregarded because it pri-
marily affects mechanical efficiency. Since the 1930s, wear
problems have prevented the normal operation of
mechanical equipment. Friction and wear are closely
related. Wear can be categorized into abrasive wear, fati-
gue wear, adhesive wear, and corrosion wear [2]. Reducing
abrasion caused during mechanical movement is vital for
extending the service life of parts, shortening the produc-
tion and processing cycles of products, and reducing
production costs [3].

Axial piston pumps offer advantages of high operating
pressure, high efficiency, long lifetime, and easy control of
variables. They are widely used in construction machinery,
ships, aerospace, and other fields. Currently, most theo-
retical studies pertaining to the wear characteristics of
piston pumps are based on the kinematic auxiliary com-
ponents of hydraulic pumps. The main reasons contributing
to the failure of piston pumps are wear, fatigue, and ageing.
Worn-out pistons, sliding shoes, and valve plates contribute
primarily to the reduced mechanical efficiency and lifetime
of the piston pump [4]. Researchers in China and abroad
have performed numerous theoretical and experimental
studies pertaining to the friction and wear characteristics of
the valve of piston pumps and obtained certain results.
Chen et al. [5] established a friction and wear prediction
model for the valve of an aviation piston pump, and Wang
et al. [6] analysed the wear characteristics of the valve of
axial piston pump at high speed. A few foreign scholars [7]

L. Xu (✉) · Y. Lu · Q. Liu · L. Lin · J. Mu
School of Electromechanical and Automotive Engineering,
Yantai University, Yantai 264005, China
e-mail: 123952467@qq.com

J Fail. Anal. and Preven. (2022) 22:738–749

739

investigated the improvement in piston pump performance using different materials as well as different cooling and lubrication methods. Many researchers worldwide believe [5-7] that understanding and analysing the wear conditions of various system components as well as determining the wear mechanism of the axial piston pump will enable more appropriate improvements.

The sliding piston shoe is one of the main friction auxiliary components in the piston pump. The slipper and the swash plate are often designed based on the principle of hydrostatic support. Ideally, an oil film is applied between them [8-10] to avoid direct contact between them. However, in practice, owing to various factors, the oil film is often destroyed, resulting in friction and wear [11, 12]. Under a large moment of inertia, the slipper is more prone to wear and abrasion because of the heavy eccentric load, which affects the lifetime of the piston pump [13]. The valve plate that constitutes the auxiliary valve is primarily designed using the method based on the residual compressive force [14, 15]. Owing to calculation errors, the valve plate often exhibits problems such as wear, biting, and disc burning [16-18]. Hence, to solve current friction and wear problems, the friction force and factors of the auxiliary slipper and valve must be investigated systematically. The friction components affect both the volumetric efficiency and mechanical efficiency. Hence, friction and wear must be understood to improve the total efficiency.

Three Main Frictional Pairs

The axial piston pump comprises three key friction pairs as follows: (i) The piston pair, which comprises a piston and a cylinder; (ii) the slipper pair, which comprises a slipper and a valve plate; and (iii) the valve pair, which comprises a cylinder and a valve plate. The most typical failure mode in piston pumps is the wear of the three above-mentioned friction pairs [19].The selection and matching of friction pair materials is one of the key factors affecting the performance and service life of piston pump. The significance of this paper is to provide basis for the selection of materials and reference for the use of piston pump.

Slipper Pair

During the operation of the axial piston pump, the slipper pair will form a certain wedge-shaped oil film relative to the surface of the valve plate under the action of the overturning moment. The pressure field of the wedge-shaped oil film of the slipper pair is always in dynamic balance with the external force and moment of the slipper under the action of the supporting force from the oil film static pressure, the effect of the oil film dynamic pressure,

and the compressive effect. The structure of the slipper pair is shown in Fig. 1. From the actual situation of pump damage, the burning of the slipper and the copper adhered onto the valve plate are main reasons contributing to pump failure [20]. The typical failure patterns of the slipper pair are shown in Fig. 2.
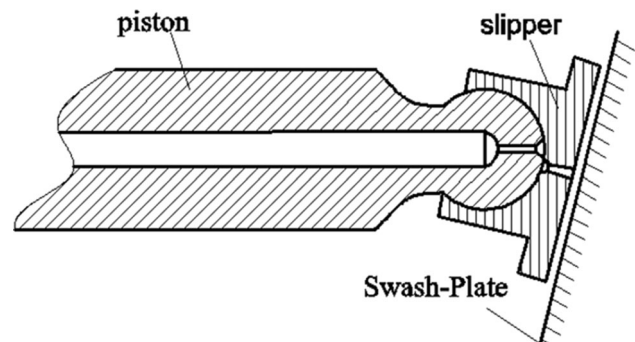
Valve Pair

The valve plate distributes oil into high-pressure and low-pressure channels in the hydraulic pump such that the pump can output high-pressure oil when the piston in the pump is in operation. On the valve plate, the vane forms a triangular slot from the oil sealing region to the oil pressure window, as shown in Fig. 3. The triangular slot allows the sealing volume between adjacent vanes to gradually enter the pressure oil window, and the pressure increases gradually, thereby eliminating oil trapping and instantaneous flow pulsation and noise caused by abrupt pressure changes [21]. The basic structure of the valve pair is shown in Fig. 4, where the compression cylinder and valve plate are shown on the left and right, respectively.

Piston Pair

Compared with the slipper and valve pairs, the movement and force conditions of the piston pair are more complicated.

From a kinematics perspective, the piston not only rotates around the centerline of the cylinder, but also randomly rotates around itself. From a dynamics perspective, the piston is subjected to the friction between itself and the cylinder, piston gravity, oil pressure, and pressure of oil film between the piston and cylinder during operation [20:8-9]. Aslanyan [22] applied a counter pressure to a high-pressure piston pair to prevent the cylinder of the piston pair from being damaged by mechanical pulling force. Calculations indicate that the counter-pressure piston has a slowdown stroke speed and a constant air pressure correction.
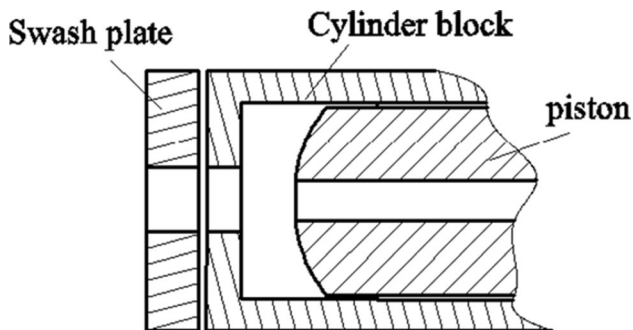

Fig. 1 The structure of the slipper pair[20-P5]

Fig. 2 The failure of the slipper pair
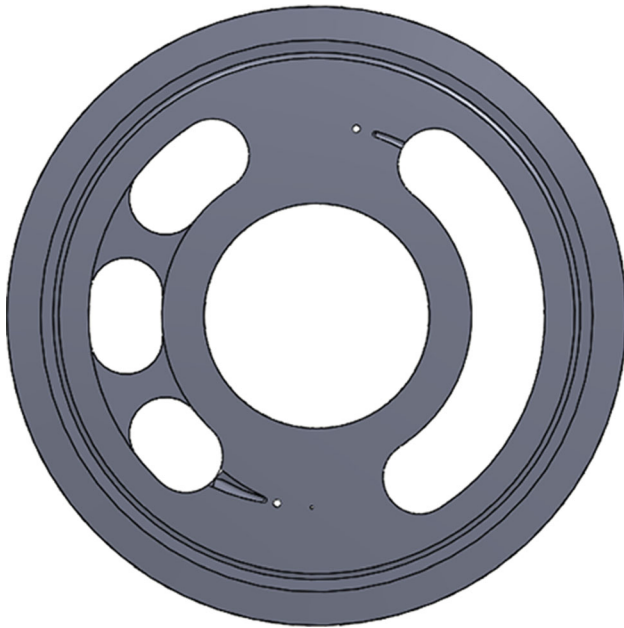
Fig. 3 The valve plate

Fig. 4 The valve pair[20-P5]

Test

Factors Affecting Coefficient of Friction

The coefficient of friction refers to the ratio of the frictional force to the positive pressure, expressed as

$$f = \frac{F}{P} \tag{Eq 1}$$

In Eq. 1, F is the frictional force [N], and P is the positive pressure force [N].

In practice, many factors affect the coefficient of friction, such as the characteristics of the material, whether a film exists on the friction surface (lubricating oil, oxide, dirt), duration of static contact, the speed at which the load is applied, stiffness and elasticity of the friction assembly, sliding speed, temperature of the friction assembly, pressure, contact characteristics, surface dimensions of objects, surface quality, and roughness.

Test Samples

In the friction and wear test for the pin–disc, the typically used wear test method in the form of planar contact is adopted [23]. For friction pairs with surface contact, owing to the low contact surface pressure, the main failure mode is adhesive wear. The friction pair is typically made of one soft material and one hard material [2]. The dimensions of the pin sample made of HMn58-2 manganese brass are shown in Fig. 5a. The pin sample exhibits good mechanical properties and is easy to process under heat. The dimensions of the disc sample are shown in Fig. 5b. Meanwhile, 20CrMo alloy steel was used to fabricate the valve plate. In the material matching of frictional pairs, copper and alloy steel are the two most commonly used materials, so these two materials are selected based on the frictional properties in pair.

Test Procedure

A Plint TE-92(Phoenix Tribology Co.,Ltd.,England) tribometer was used to test the friction and wear characteristics of the pin–disc under different load and speed conditions. A Zeiss microscope was used to observe the microstructure and morphology of the pin–disc after wear. The test parameters were: the speed was increased by 100RPM and the load was increased by 50N every two minutes. The test samples were categorized into four
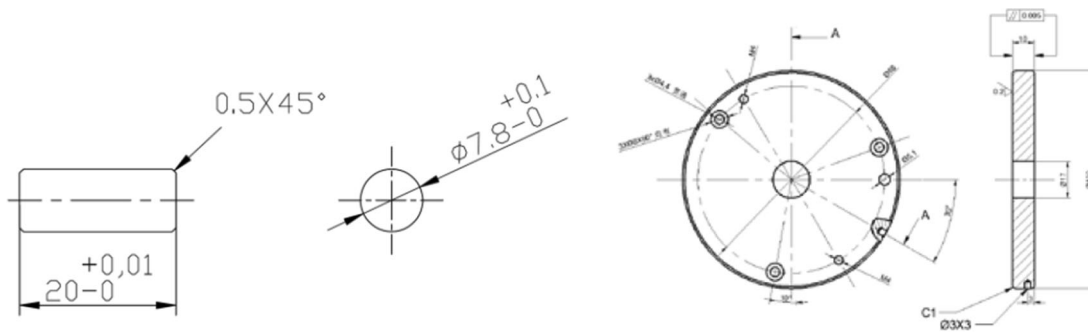
(a) The dimension of the pin sample **(b)** The dimension of the disc sample

Fig. 5 The dimensions of the pin–disc sample

Fig. 6 The test equipment and disc sample

(a) The appearance of the test equipment **(b)** The appearance of the disk sample

groups, which comprised one group for the dry friction test, and three groups for the lubricated friction test using no. 46 anti-wear hydraulic oil. The same processing technology was used for each group, and the sample radius was standardized to 30 mm. Figure 6 shows the test equipment with the Plint TE-92 tribometer and pin–disc, where Fig. 6a and b shows the appearance of the Plint TE-92 test equipment and disc sample, respectively.

Analysis of Test Results

Dry Friction Test

The speed, pressure, and time of the pin–disc tests can be set through the Plint TE-92 tribometer. Figure 7 shows the change in the coefficient of friction during the test when the dry friction. In the dry friction test, the increase in pressure and speed will cause the frictional force to increase significantly and the coefficient of friction to increase
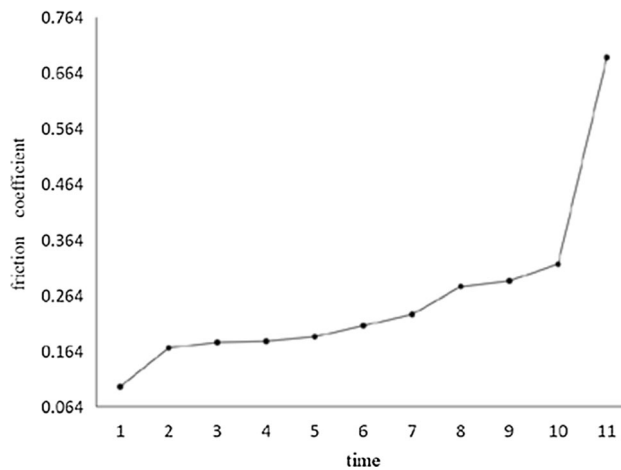

Fig. 7 The change in the coefficient of friction when the dry friction

accordingly. As the testing equipment began to rotate, noise due to friction was audible during the acceleration process. At the 11th second, when the speed increased to

2,350 rpm and the pressure increased to 200 N, the coefficient of friction increased to 0.691, and the testing equipment generated a harsh friction sound. To avoid equipment damage and to ensure safety, the test was terminated.

Macroscopic Observation

Photographs of the physically worn pin–disc are shown in Figs. 8 and 9. As shown in Fig. 8, the sample surface exhibited friction marks. The relatively high speed increased the temperature of the friction surface, and consequently, the friction pair became more prone to wear at high temperatures. The pin was made of brass. The high temperature of the experiment resulted in a few copper particles accumulating and adhering on the surface of the disc in the form of flakes; consequently, round marks with a slightly yellow circumference appeared because of friction. The wear of the three pins was not uniform.

The surface morphology of the worn sample was observed using a Zeiss microscope. A furrow appeared on the contact surface of the copper pin, and scratches arranged in a regular pattern were observed. The abrasion increased the surface roughness of the disc, as shown in Fig. 10a. The contact surface was worn significantly, and the scratches were staggered. As shown in Fig. 10b, a few particles remained because of the copper pin. From the photomicrograph of the pin–disc after the dry friction test, as shown in Fig. 10, the scratches of the pin were lighter than those of the disc.
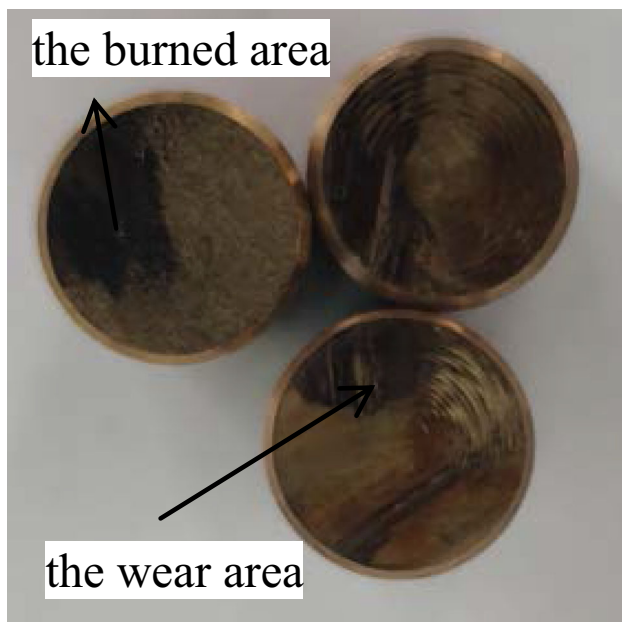
Anti-Wear Hydraulic-Oil-Lubricated Friction Test 1

A lubricated friction test using No. 46 anti-wear hydraulic oil was first performed, and the speed was increased from 400 to 1,700 rpm. Figure 11 shows the change in the coefficient of friction during the test when the rotational speed was maintained at 1,100 rpm. The speed was fixed at 1,100 rpm, whereas the load was added incrementally; the coefficient of friction first increased and then decreased. When the load was 1120 N, the maximum coefficient of friction was 0.086. When the pressure was increased to 700, 1,100, 1,300, and 1,400 N, the average coefficient of friction values were 0.08116, 0.08169, 0.08065, and 0.07922, respectively. At the rotational speed of 1100 rpm, the difference in the coefficient of friction under different loads was insignificant. A greater load did not correspond to a larger coefficient of friction.

During the test, the load and speed were constantly changing with time. Figure 12 shows the change in the coefficient of friction with varied rotate speed, Fig. 13 shows the change in the average coefficient of friction at different speeds and loads over time during all tests. At the beginning of the test, the test equipment has not yet entered a stable state; hence, the measured coefficient of friction was relatively large and fluctuated significantly. After the equipment operated stably, the coefficient of friction stabilized and changed regularly. During the test, the speed was fixed first, and the load was added incrementally; subsequently, the speed was increased, and the load was added incrementally again. The experiment was performed as such reciprocally. As shown in Fig. 13, the coefficient of

Fig. 8 The wear map of three test pins

Fig. 9 The wear map of test disc

(a) pin **(b)** disc
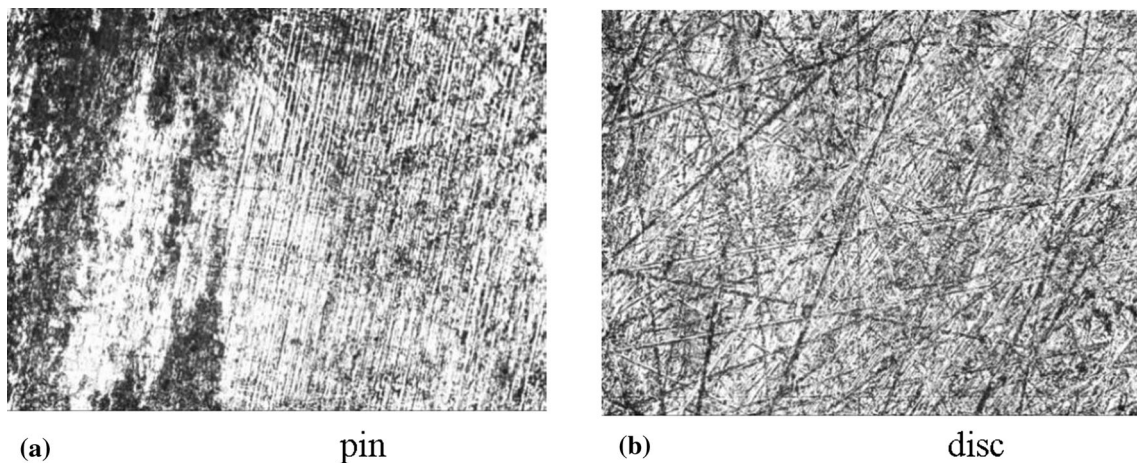
Fig. 10 The photomicrograph of the pin–disc after the dry friction test (200X)
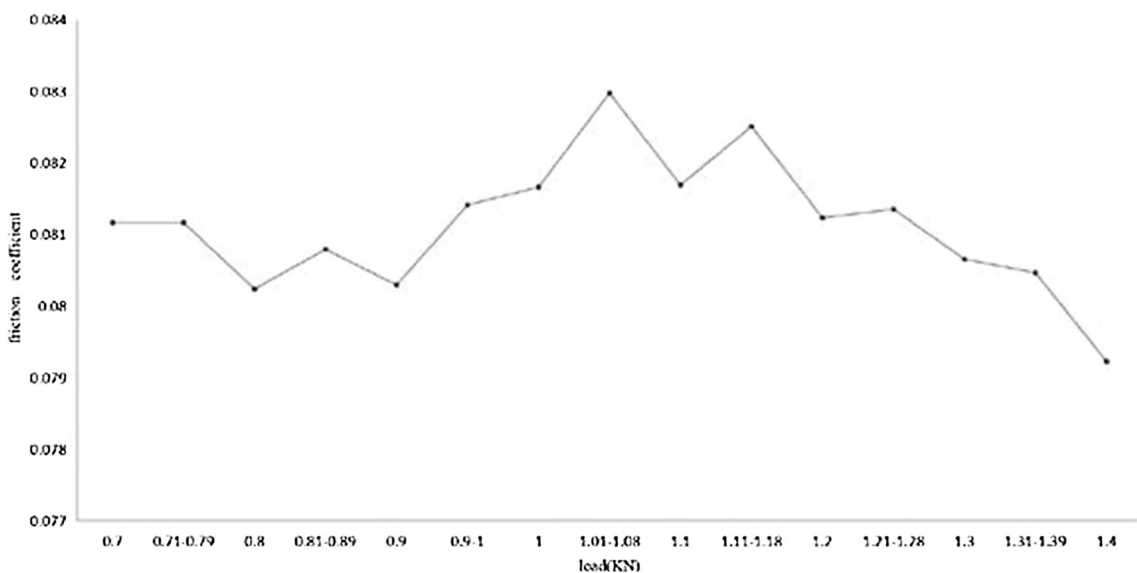
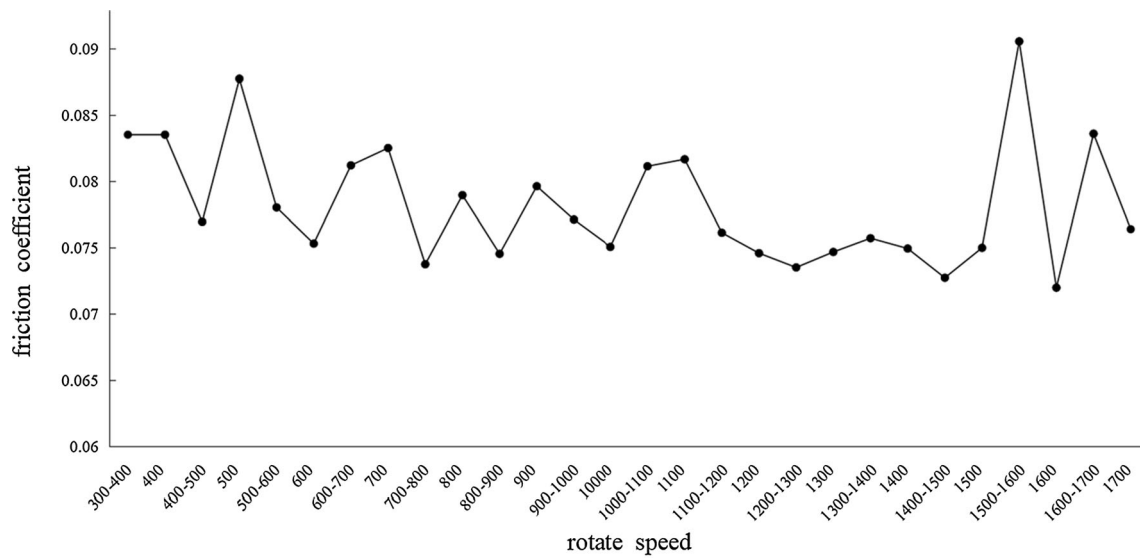Fig. 11 The change in the coefficient of friction when the rotational speed at 1,100 rpm

friction showed a trend of first increasing and then decreasing, followed by increasing and then decreasing. When the test was about to be terminated, the speed and load decreased, and the coefficient of friction decreased as well. Furthermore, 5s before the equipment stopped operating completely, the coefficient of friction increased abruptly. It was speculated that the pin–disc may have been hit, causing the oil film between the pin and disc to be destroyed; therefore, the pin–disc contact surface resulted in dry friction in the absence of lubricating oil.

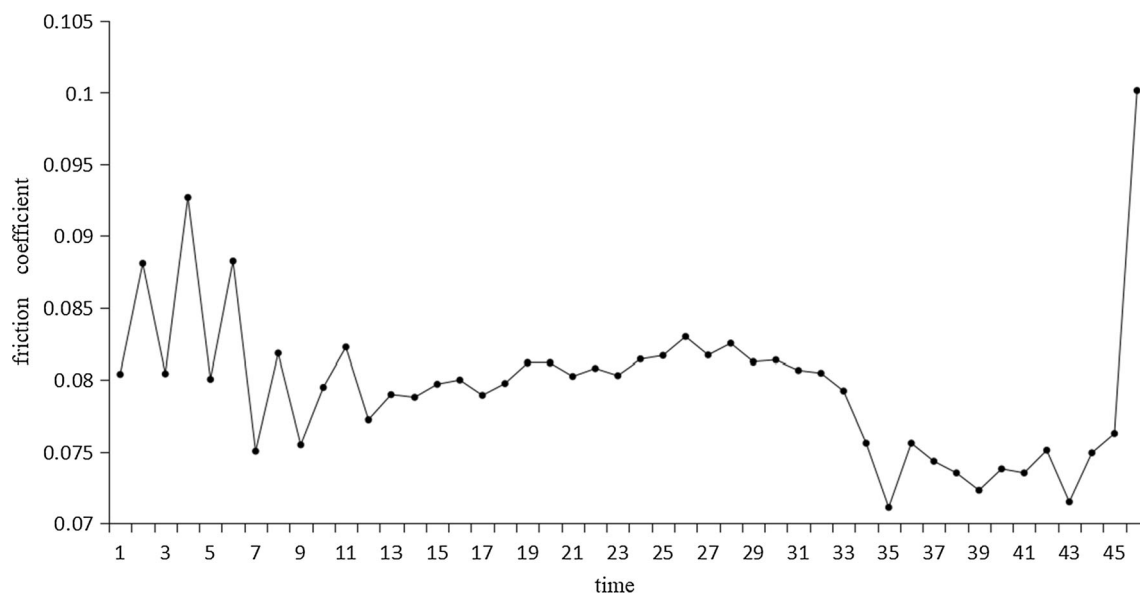Anti-Wear Hydraulic-Oil-Lubricated Friction Test 2

In the second lubricated test using No. 46 anti-wear hydraulic oil, the load was increased from 1,100 to 1,410 N. Figure 14 shows the change in the coefficient of friction

during the test when the load was maintained at 1,100N. The load was fixed at 1,100 N and the speed was increased incrementally. When the speeds were 1,100, 1,300, 1,600, and 1,998 rpm, the average coefficient of friction values were 0.0804, 0.0789, 0.0842, and 0.1289, respectively, and the load reached the critical value at 1,200 N. When the load was fixed and the speed was increased, the coefficient of friction first decreased and then increased.

Figure 15 shows the change in the average coefficient of friction at different speeds over time during all tests. At the beginning of the test, owing to the relatively small load, the coefficient of friction was relatively small as well. When the load increased to 1,300 or 1,400 N, the coefficient of friction began exhibiting an upward trend. When the rotation speed was 2,000 rpm and the load was 1.1 KN, the maximum coefficient of friction was reached, i.e., 0.147. It

Fig. 12 The change in the coefficient of friction with varied rotate speed

Fig. 13 The average friction coefficient varied with load and speed throughout the test

can be assumed that these conditions caused the onset of oil film damage. In practice, operating at a load of 1,300 or 1,400 N and a rotational speed of 1,600–2,000 rpm should be avoided. As the friction test progressed, the temperature of the test equipment and the sample material continued to increase; simultaneously, the speed continued to increase, causing the coefficient of friction to exhibit a downward trend.

Anti-Wear Hydraulic-Oil-Lubricated Friction Test 3

In the third lubricated test using No. 46 anti-wear hydraulic oil, the load was increased from 500 to 1,400 N, and the

speed was increased from 300 to 2,100 rpm. The rotational speed was maintained at 500 rpm, the load was added incrementally, and the coefficient of friction changed, as shown in Fig. 16. Because the overall time during the third test was shorter than the first test, the coefficient of friction increased overall with a fixed speed and increasing load.

The load was maintained at 1,400 N, the speed was increased incrementally, and the coefficient of friction changed, as shown in Fig. 17. As the rotational speed increased, the coefficient of friction exhibited a downward trend, which is consistent with the second test.

Figure 18 shows the change in the average coefficient of friction at different speeds and loads over time during the
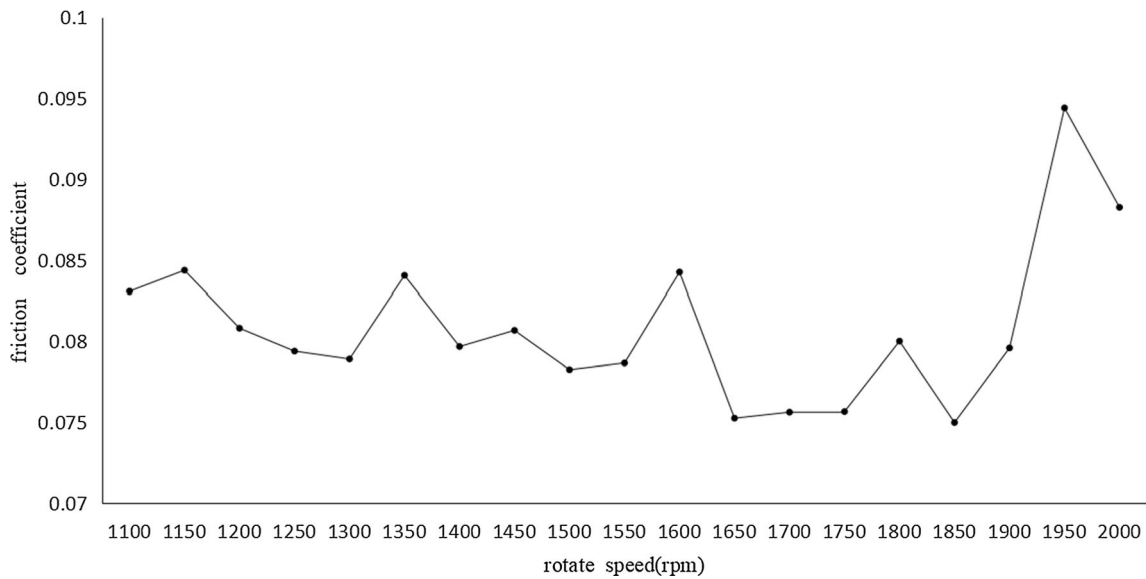
Fig. 14 The change in the coefficient of friction when the load was maintained at 1,100N
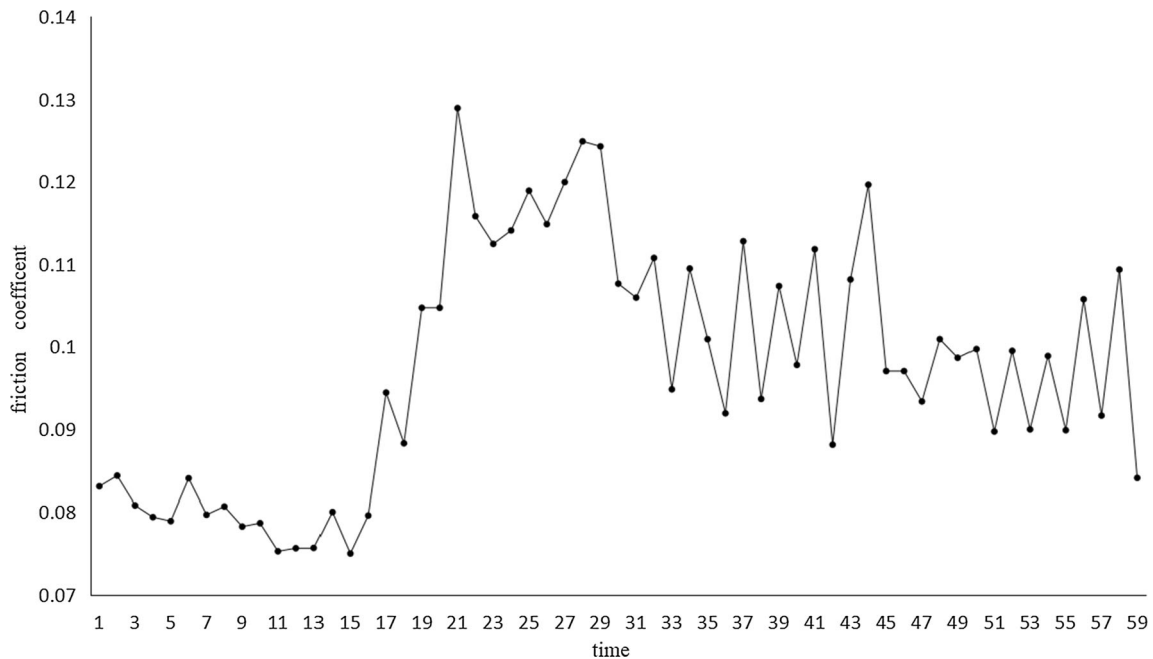

**Fig. 15** The change in the average coefficient of friction at different speeds during all tests

third test. The time required for the third test was much shorter than those of the previous two test; hence, the amount of test data corresponding to the load and speed were relatively small. It was observed from the figure that as the test progressed, the load increased, whereas the speed remain unchanged, and the coefficient of friction first increased significantly. When the test was continued for one third of the total time, the load and speed changed in the same manner as in test 1. The load remained the same, whereas the speed increased significantly, thereby

significantly reducing the coefficient of friction. Subsequently, the rate at which the rotational speed increased was greater than the rate at which the load changed, and the coefficient of friction tended to oscillate and decrease. Obviously, the change of friction coefficient in Fig. 18 was consistent with the speed change trend shown in Fig. 17, but there was a large gap with the load change trend shown in Fig. 16. It was reasonable to think that under the condition of hydraulic oil, the influence weight of speed on friction coefficient was higher than that of load. To reduce

746

J Fail. Anal. and Preven. (2022) 22:738–749
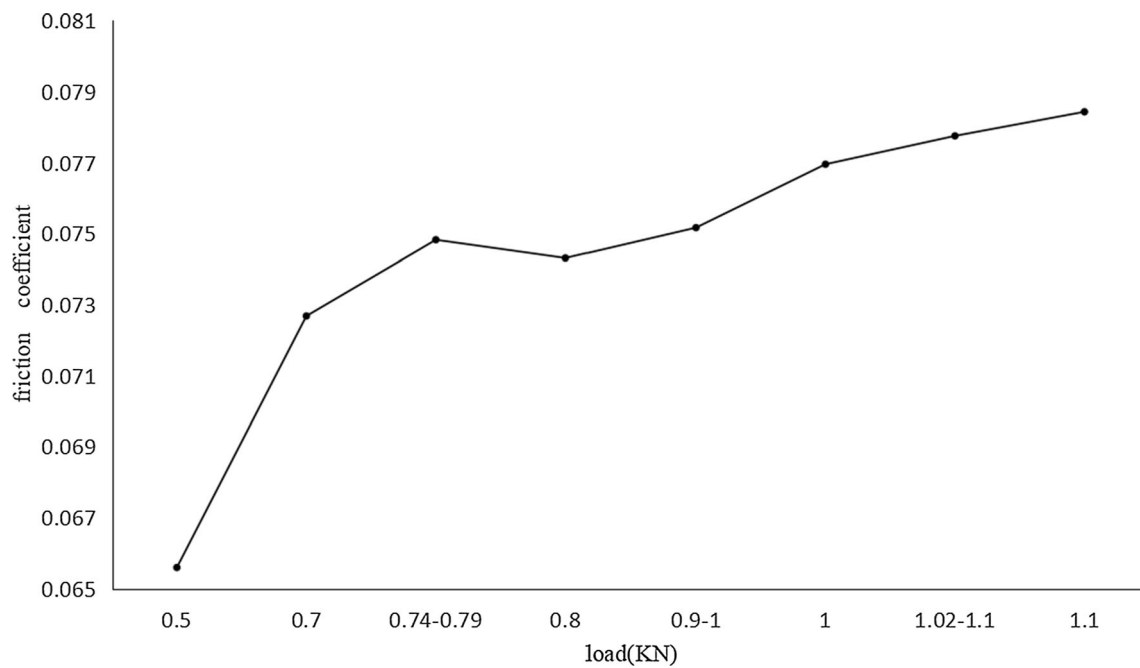
Fig. 16 The rotational speed was maintained at 500rpm
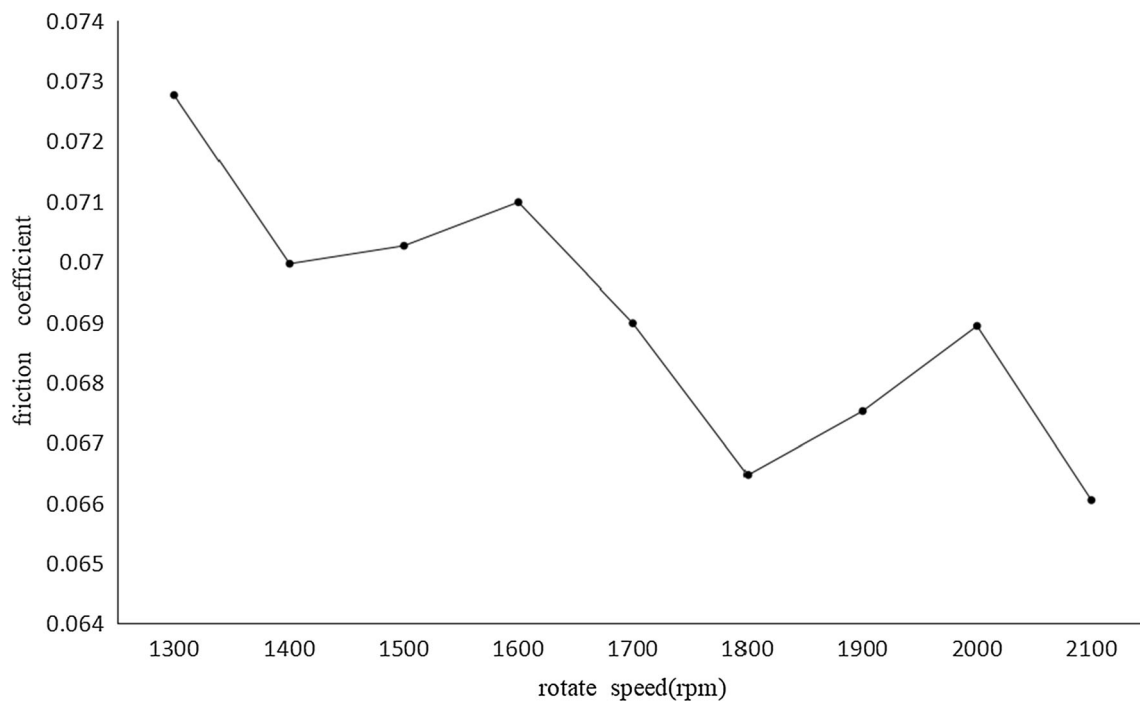

Fig. 17 The load was maintained at 1,400 N

the friction coefficient, the speed reduction should be considered first in the design of piston pump.

A photograph of the physical pin–disc after the friction test is presented in Fig. 19. As shown in Fig. 19, a clear burn mark remained on the surface of one of the pins; however, it may be residue from the lubricating oil at high temperature. In addition, one of the pins showed more serious wear, suggesting an uneven load distribution. As this pin experienced a large force in a small contact area, its wear was more severe. The light-coloured area in Fig. 19 shows the wear. The band in the friction zone on the surface of the disc presents a yellow colour, which was due to
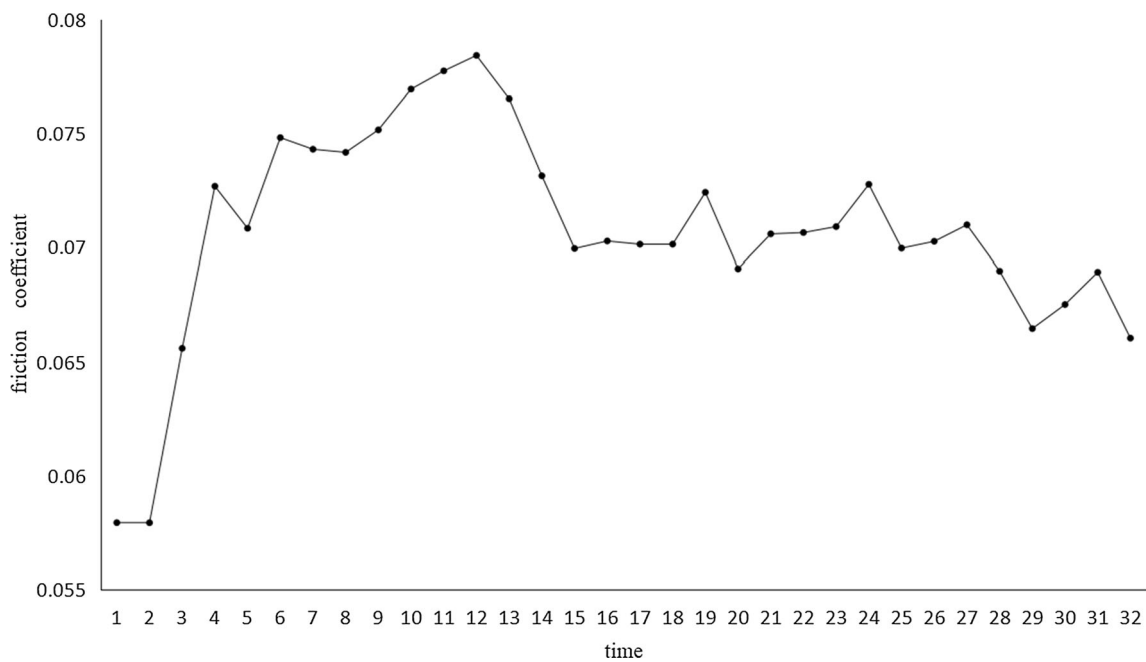
Fig. 18 The change in the average coefficient of friction at different speeds and loads

Fig. 19 Photographs of the physical pin–disc after the friction test

**(a)**   pins

(b)   disk
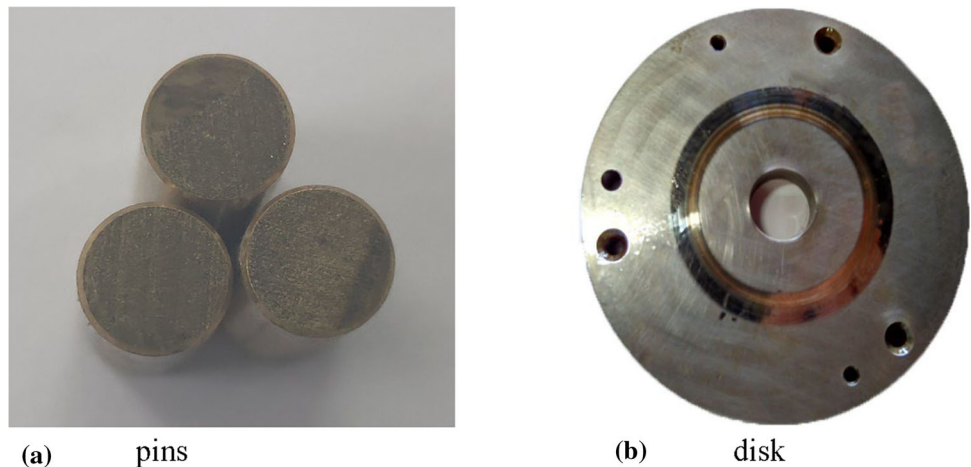
the adhesion of copper, indicating that the temperature in this area was relatively high. The outer band showed a bright metallic colour. Based on the photomicrograph shown in Fig. 20, the wear marks were relatively regular and normal. The wear was primarily abrasive wear in the form of furrows, with supplementary adhesive wear.

Conclusions

(1) In the dry friction test, the pin–disc was worn unevenly, causing the equipment to be damaged easily. Dry friction should be avoided as much as possible in the friction test and in actual production. In the friction test using no. 46 anti-wear hydraulic oil lubrication, when the load was 1,400 N, the speed was 1,300–2,100 rpm, the coefficient of friction was less than 0.073, and the test equipment operated smoothly. When the load was between 1,300 and 1,400 N, and the speed was 1,600–2,000 rpm, and the coefficient of friction was greater than 0.011, indicating the onset of oil film damage. In practice, these parameter ranges should be avoided in actual application.

(2) Pressure P and speed V are the key parameters in the design and use of piston pump. The test parameter load in this paper can be converted into P value, and the speed in the test can be converted into V value. Therefore, the test parameters in this paper provide a

748

J Fail. Anal. and Preven. (2022) 22:738–749

(a) pin   **(b)** disk
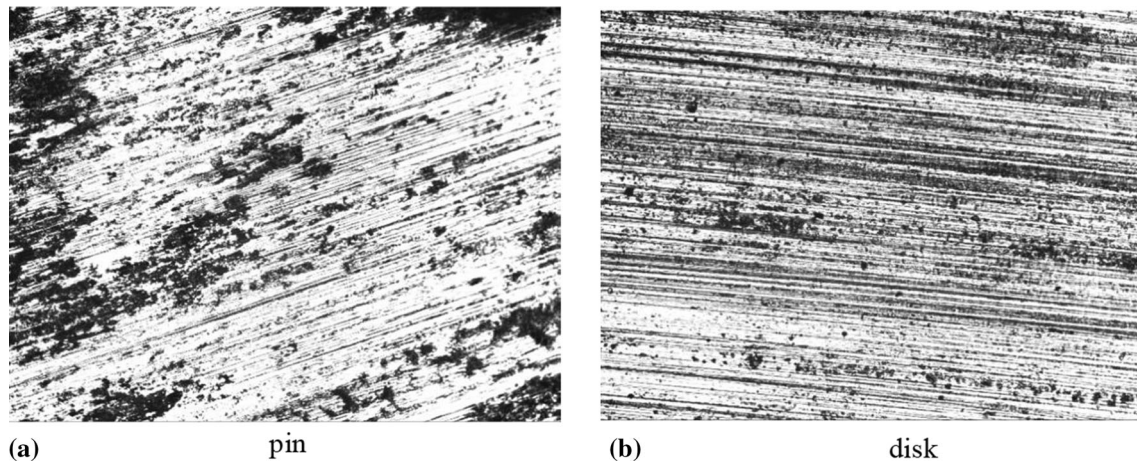
Fig. 20 Photomicrographs of pin and disc (200X)

certain reference for the parameter design and use of piston pump.

(3) A greater speed resulted in a smaller coefficient of friction, whereas a greater load resulted in a greater coefficient of friction. Meanwhile, a higher temperature resulted in a smaller coefficient of friction. The effect of speed on the coefficient of friction was slightly more prominent than the effect of load.

References

1. G. Schuhler, A. Jourani, S. Bouvier et al., Wear mechanisms in contacts involving slippers in axial piston pumps: a multi-technical analysis. J. Mater. Eng. Perform. **27**(3), 5395–5405 (2018)
2. S, Wen, H. Ping. Principles of Tribology.Tsinghua University Press, 2012. P284
3. H. Yuhao, H. Ping, Experimental analysis of a numerical calculation method of wear. Lubr. Eng. **44**(6), 10–16 (2019)
4. Ma. Jiming, H. Yihong, G. Jian et al., Review of wear analyses research for main moving pairs in hydraulic axial piston pump. Chinese Hydraulics & Pneum. **000**, 84–94 (2017)
5. C. Yuanling, B. Chengzhou, L. Yinshui et al., Wear model and life prediction of port pair in aircraft piston pump. Chinese Hydraulics & Pneum. **12**, 1–7 (2020)
6. Wu. Wang Zhenglei, H.J. Yucheng, The high speed tribological performance of port plates in axial piston pumps. Chinese Hydraulics & Pneum. **8**, 27–32 (2019)
7. R.K. Gunda, S. Narala, Evaluation of friction and wear characteristics of electrostatic solid lubricant at different sliding conditions. Surface and Coatings Technol. **332**, 341 (2017)
8. M. Jiajia, H. Zhiying, L. Baolin, The analysis on the slipper pair's hydrostatic back-up of swash plate axial piston pump. Hydraulics Pneum. & Seal. **3**, 70–71 (2018)
9. S. Hongmei, L. Jianxun, Y. Mengxue et al., Analysis of film lubrication properties for swash plate pump slipper in the process of intensely wear working condition. Chinese Hydraulics & Pneum. **2**, 5–10 (2017)
10. T. Hesheng, L. Jing, Y. Yaobao et al., Research development of thermohydrodynamic lubrication of slipper / swash plate pair in axial piston pump. Mach. Tool & Hydraulics. **44**(9), 153–160 (2016)
11. J. Ma, J. Chen, J. Li et al., Wear analysis of swash plate/slipper pair of axis piston hydraulic pump. Tribol. Int. **90**, 467–472 (2015)
12. L. Xu, H. Sun, S. Xu, Fracture mechanism analysis on the slipper retainer in axial piston pumps. Eng Failure Anal. **80**, 378–385 (2017)
13. G. Peipei, N.X. WangRui et al., Friction and wear properties of C67300 manganese brass under oil lubrication for application in piston pumps. The Chinese J. Nonferrous Metals. **30**(12), 2920–2929 (2020)
14. X. Bing, Y.-h Sun, J.-h Zhang, A new design method for the transition region of the valve plate for an axial piston pump. Appl. Phys. Eng. **16**(3), 229–240 (2015)
15. H. Yang, Q. Ai, H. Zhou, Development of lubrication of port plate/cylinder block in axial piston pump. China Mech. Eng. **15**(17), 1587–1593 (2004)
16. R. Shen, L. Pengfei, Research on Friction Performance Study of Piston Pairs of Swash PlateAxial Piston Pump and Port Plate Pair. Mach. Design & Manufacture. **4**, 36–39 (2014)
17. X. Chen, A study on the low-speed tribological performance of port plates in axial piston pumps. Zhejiang University, 2017(3)
18. C. Xubin, G. Xiang, Z. Yi et al., A study on microstructure and tribology performance of samples processed by selective laser melting. Chinese J. Mech. Eng. **54**(3), 63–72 (2018)
19. Z.H.A.O. Jian-hua, L.I.U. Hang, W.A.N.G. Xin-wei et al., Analysis on transfer path of fluid vibration of swash plate axialplunger pump under failure mode. Mach. Tool & Hydraulics. **48**(6), 1–9 (2020)
20. Li. Jing, Fundamental theory and application of thermal analysis for hydraulic piston pumps. Mach. Design & Res. **03**, 206 (2017)
21. S. Wang, The analysis of cavitation problems in the axial piston pump. J Fluid Eng. **7**(132), 0745021–0745026 (2010)
22. A. Aslanyan, Dependence of the characteristics of a high-pressure piston pair on the properties of PES-3 working fluid and the pressure distribution in the piston-cylinder gap. Meas. Tech. **10**, 811–815 (2021)
23. Q. Shaojun, X. Wang, D. Qian, Study on factors of pin-on-disc wear testing. Thermal Spray Technol. **7**(003), 41–47 (2015)

J Fail. Anal. and Preven. (2022) 22:738–749

749

24. Y. Guanxin, N. Huawe, Effects of nickel on tribological wear properties of copper-based powdermetallurgy friction material. Hot Working Technol. **45**, 121–124 (2016)